Bio-Design and Manufacturing (2022) 5:305–317
https://doi.org/10.1007/s42242-021-00152-5

RESEARCH ARTICLE

Electrospinning of a sandwich-structured membrane with sustained release capability and long-term anti-inflammatory effects for dental pulp regeneration

Fenghe Yang[1] · Jiangxue Wang[1] · Xiaoyu Li[1] · Zhenzhen Jia[1] · Qiang Wang[2] · Dazhi Yu[3] · Jinyu Li[4] · Xufeng Niu[1]

Received: 7 January 2021 / Accepted: 12 June 2021 / Published online: 1 September 2021

Abstract

Current electrospun membranes used for pulp capping still lack the sustained-release capability and long-term anti-inflammatory effects that are favorable for dental pulp regeneration. In this work, a single-layered poly(lactic acid) (PLA) electrospun membrane loaded with amorphous calcium phosphate (ACP) and aspirin (PLA/ACP/Aspirin membrane, i.e., PAA membrane) is sandwiched between two poly(lactic-co-glycolic acid) (PLGA) electrospun membranes as a novel sandwich-structured PLGA and PAA composite electrospun membrane (PLGA-PAA membrane) to resolve the need for sustained-release design and anti-inflammatory effects. Contact angle measurements indicate that the PLGA-PAA membrane is more hydrophilic than the PAA membrane. An in vitro release study reveals that PLGA membranes coated on PAA membrane could slightly slow down ion release, while significantly prolonging aspirin release. We also co-cultured membranes with dental pulp stem cells (DPSCs) and human monocytic THP-1 cells to evaluate their osteogenic ability and anti-inflammatory effects, respectively. Compared with the PAA membrane, the PLGA-PAA membrane promotes cell adhesion, proliferation, and osteogenic differentiation. A prolonged anti-inflammatory effect of up to 18 days is also observed in the PLGA-PAA group. The results suggest a promising strategy for fabricating an electrospun membrane system with controlled release capabilities and long-term anti-inflammatory effects for use as pulp-capping material for regeneration of the dentin-pulp complex.

✉ Jinyu Li
leery_5566@163.com

✉ Xufeng Niu
nxf@buaa.edu.cn

[1] Key Laboratory for Biomechanics and Mechanobiology of Ministry of Education, Beijing Advanced Innovation Center for Biomedical Engineering, School of Biological Science and Medical Engineering, Beihang University, Beijing 100083, China

[2] Department of Burn Plastic Surgery, 80th Army Hospital of PLA, Weifang 261021, China

[3] Department of Hand Surgery, 971st Army Hospital of PLA, Qingdao 266000, China

[4] Department of Orthopaedics, Dongzhimen Hospital, Beijing University of Chinese Medicine, Beijing 100700, China

Graphic abstract

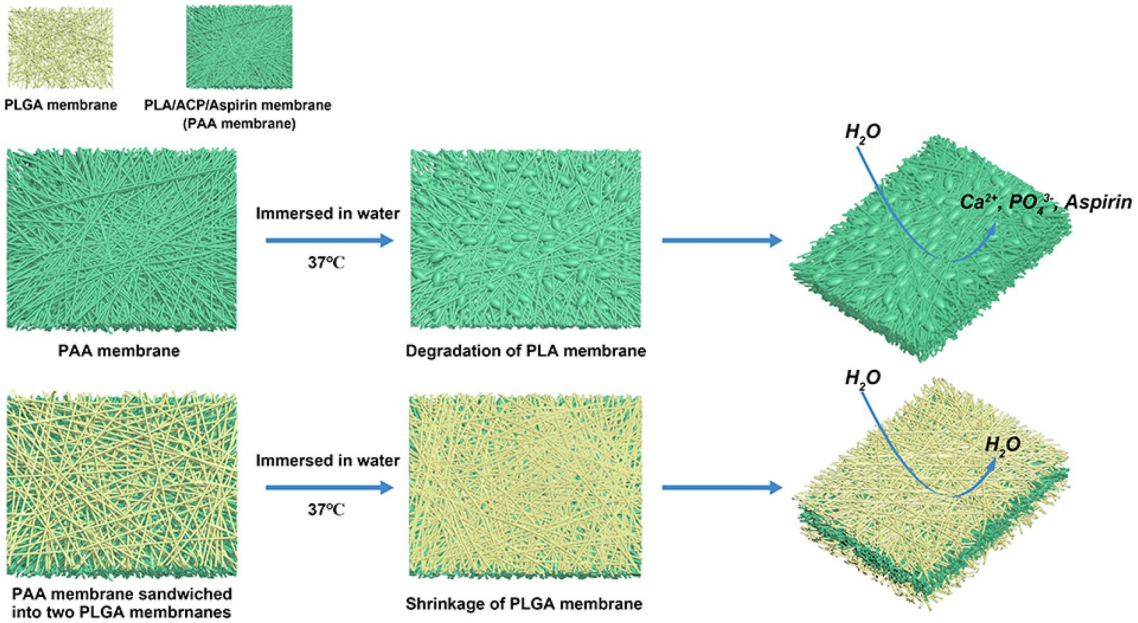

Keywords Electrospinning · Sandwich-structured · Pulp capping · Controlled release · Anti-inflammatory effects

Introduction

Dental pulp is a well innervated, vascularized tissue located in the central portion of the tooth [1], surrounded by dentin and composed of collagen fiber, fibroblasts and dental stem cells [2]. Living pulp is the guarantee of dental health. However, exposure of vital pulp may sometimes occur, due to dental caries or trauma, resulting in dentin loss and pulp injury [3]. To restore the vitality of pulp and stimulate dentin formation, pulp-capping materials can be added to the exposed pulp [4, 5].Various materials like calcium hydroxide, mineral trioxide aggregates, and resin-based cements have been used as pulp capping material [6–10]. However, most of these materials lack biocompatibility and may irritate the pulp tissue, resulting in chronic pulp inflammation, which is unfavorable for pulp regeneration and dentin formation [11–13].

Recent studies have shown that electrospun membranes are promising candidates for pulp capping [14, 15], as these materials have many advantages over traditional materials. First, these membranes mimic the natural extracellular matrix (ECM) of pulp tissue [16–18]. The nanofiber in the electrospun membrane possesses a similar diameter to collagen type I (Col I), while Col I is the most abundant extracellular protein in dentin and the base for primary and reparative dentin formation [19, 20]. Second, biocompatible polymers can be easily processed into nanofibrous structured membranes through electrospinning techniques to obtain a pulp capping material with good biocompatibility [2, 4, 21]. Furthermore, many drugs and bioactive agents favorable to pulp regeneration and dentin formation can be also incorporated into the membrane for an enhanced therapeutic effect [22, 23].

Despite all the advantages listed above, there are still some deficiencies in existing electrospun membranes that limit their therapeutic effect. First, current electrospun membranes usually do not contain anti-inflammatory reagents. As is well known, pulp injury is always accompanied by an inflammatory response. This inflammatory process is not only harmful to the recovery of pulp activity [15, 24]; it also has adverse effects on bone formation (i.e., dentin formation) if the inflammatory response persists and becomes chronic [25–30]. Second, regeneration of the dentin-pulp complex is a long-term process, which also requires long-term release of any added drugs or bioactive agents during regeneration. However, the electrospun membranes currently used for pulp capping are all designed with a simple structure, which is incapable of controlled release. The drugs and bioactive agents in current electrospun membranes are always quickly released in the first few days, which may result in poor dentin-pulp complex regeneration in the late stage.

To enhance the therapeutic effects of these membranes, a new biocompatible electrospun membrane should be designed with a sustained drug/bioactive agent release capability to suppress long-term pulp inflammation as well as enhance dentin formation. Our previous work described

the synthesis of a single-layered electrospun membrane consisting of poly(lactic acid) (PLA) and amorphous calcium phosphate (ACP) [31]. This PLA/ACP membrane has been shown to be effective in inducing bone formation, as ACP can be converted in aqueous solution into hydroxyapatite (HA), the main mineral component in natural bone, with sustained release of calcium (Ca^{2+}) and orthophosphate (PO_4^{3-}) ions [32]. However, this membrane lacks the anti-inflammatory and controlled release ability necessary for successful dental pulp regeneration. As a classic nonsteroidal anti-inflammatory drug, aspirin has been proved effective in treatment of periodontitis, showing its promising application in suppressing dental inflammation [33, 34]. Owing to its solubility in electrospinning solution, aspirin can be easily incorporated into the PLA/ACP membrane as a PLA/ACP/Aspirin membrane (PAA membrane) to enhance its anti-inflammatory properties. Multilayering electrospinning is a technique with a sequential spinning process that can produce a multilayered fiber membrane [35]. Studies have shown that sequential drug release can be achieved by adding drugs onto different layers of the membrane, indicating the potential of the multilayered membrane for drug-controlled release [36, 37]. The outer layer of the multilayer membrane has an inhibitory effect on drug release; thus, by sandwiching the drug-loaded layer between two non-drug-loaded layers, a prolonged drug release time can be achieved. As a biocompatible material approved by the U.S. Federal Food and Drug Administration (FDA), poly(lactic-co-glycolic acid) (PLGA) might potentially be an appropriate material for use as the outer layer to achieve prolonged drug release capability. PLGA has similar characteristics but stronger hydrophilicity compared with PLA, making it more compatible with cells and tissues [38]. Furthermore, the solution used for PLA and PLGA electrospinning is the same, which would make the layers in the resulting multilayered membrane more tightly combined with each other. To the best of our knowledge, the multilayering electrospinning technique has never before been used in dental pulp regeneration, and the mechanism by which the outer layer influences the drug release profiles has also not been fully investigated.

The aim of this study is to fabricate a sandwich-structured PLGA and PAA composite electrospun membrane (PLGA-PAA membrane) for use in dental pulp regeneration through a multilayering electrospinning technique, in which the PAA electrospinning membrane is set as the inner layer while the two PLGA electrospinning membranes are set as the outer layers. In order to better validate the release inhibition effect of the PLGA membrane, we selected PLA with low molecular weight to fabricate a PAA membrane with fast-release properties. We hypothesized that after being sandwiched between the PLGA membranes, the PLGA-PAA sandwich-structured membrane would achieve a prolonged drug/bioactive agent release time and long-term anti-inflammatory effects, which are more favorable to dental pulp regeneration. To test this hypothesis, we carried out in vitro degradation studies, in vitro release studies, cell differentiation assays and in vitro anti-inflammation experiments.

Materials and methods

Materials

PLA (RESOMER R 207 H, Inherent viscosity: 0.25–0.35 dL/g) and PLGA (RESOMER RG 503 H, Inherent viscosity: 0.32–0.44 dL/g, LA/GA = 50:50) were purchased from Evonik Industries AG (Essen, Germany). Aspirin was donated by Dr. Zhongning Liu from Peking University Hospital of Stomatology. $Ca(NO_3)_2{\cdot}4H_2O$ and $(NH_4)_2HPO_4$ were purchased from Sinopharm Chemical Reagent Co., Ltd. (Beijing, China). Dichloromethane (DCM) and N,N-Dimethylformamide (DMF) were obtained from Beijing Tongguang Fine Chemicals Company (Beijing, China).

Preparation of PAA electrospun membrane

ACP was first synthesized using a wet chemical method as previously described [32]. A polymer solution containing 50% w/v PLA with aspirin at 1.75 wt% PLA was then prepared in a 3:1 DCM: DMF solvent mixture. After the above ingredients were dissolved, ACP powders at 10 wt% PLA were added, and the solution was stirred for 1 h to create a uniform suspension of ACP. The solution was then loaded into a 20 mL syringe and electrospun at 20 kV under a steady flow rate of 1.2 mL/h for 2.5 h. The distance between the syringe needle and the collection foil was 10 cm. After electrospinning, the resulting PAA electrospun membrane was collected and dried in a desiccator overnight. The dried PAA electrospun membrane was cut into small pieces of equal weight for use in further experiments.

Preparation of PLGA-PAA electrospun membrane

A PLGA solution with a concentration of 30% w/v was prepared by dissolving PLGA in DCM and DMF mixed solvent at a ratio of 3:1. The solution was transferred into a 20 mL syringe and electrospun at 20 kV under a steady flow rate of 1.6 mL/h. The distance between the syringe needle and the collection foil was 10 cm. Before electrospinning, the small pieces of PAA prepared earlier were first adhered to the collection foil by electrostatic interaction. Both sides of the PAA membrane were electrospun for 1 h to distribute PLGA fibers uniformly across its surface. The resulting PLGA-PAA membranes were collected and dried in a desiccator overnight.

Characterization of electrospun membrane

The surface and cross-sectional appearance of electrospun membranes was observed under a scanning electron microscope (SEM) (FEI Quanta 250 FEG, USA). Samples were coated with platinum before viewing. An energy-dispersive spectrometer (EDS) was employed to analyze the chemical composition of membranes. In addition, the diameter distribution of nanofibers was also tested using the image analysis program ImageJ (National Institute of Health, Bethesda, USA).

Contact angle

To determine the hydrophilicity of the membranes before and after coating with PLGA nanofibers, the contact angle of each sample was measured with a contact angle measurement system (JC2000FM, POWEREACH, China). The water droplet size was set as 0.5 μL, and the final result for each sample was obtained by averaging five separate runs.

Thermal analysis

A thermogravimetric analyzer (NETZSCH STA 449 C Jupiter, Germany) was used for thermogravimetric analysis (TGA) to determine ACP loading efficiency of different membranes. Samples with an average weight of 10 mg were placed in alumina crucibles and measured under a nitrogen atmosphere (50 mL/min) at temperatures ranging from room temperature to 800 °C at a heating rate of 10 °C/min. Differential scanning calorimetric (DSC) analysis (NETZSCH STA 449 F5 Jupiter, Germany) was also conducted to test the inherent properties of PLGA. DSC runs were carried out over a temperature range of 25–200 °C at 10 °C/min under dry nitrogen flow (50 mL/min).

In vitro degradation studies

In vitro degradation studies were carried out by monitoring mass loss and surface morphology of electrospun membranes over a period of 28 days. Twenty milligrams of membranes were placed in a test tube, immersed in 3 mL of phosphate-buffered saline (PBS) (0.1 M, pH 7.4), and maintained in a 37 °C-incubator shaker. At predetermined time intervals, membranes were collected and lyophilized for 24 h. The mass and morphology of each membrane were assessed with an electronic balance and SEM, respectively.

In vitro release studies

In vitro release studies were performed by measuring ion release (Ca^{2+}, PO_4^{3-}) and aspirin release over a period of 35 days. Twenty milligrams of electrospun membranes were placed in test tubes, immersed in 3 mL of physiological saline, and kept in a 37 °C-incubator shaker. At predetermined time intervals, all of the medium was collected for testing and replaced with an equal amount of fresh physiological saline. The concentrations of calcium ion and phosphate ion released into the test solution were measured by a calcium colorimetric assay kit (Sigma-Aldrich, USA) and phosphate ion colorimetric assay kit (Sigma-Aldrich, USA), respectively, using manufacturers' protocols.

Before measuring in vitro aspirin release, a preliminary acceleration experiment was conducted to calculate the encapsulation efficiency of aspirin in the electrospun membrane. Briefly, twenty milligrams of membranes were placed in test tubes, immersed in 3 mL of PBS, and maintained in an incubator at 60 °C and 150 r/min. When the membranes were totally degraded, the supernatants in each tube were collected, and the amount of aspirin in the supernatants was tested using a multimode microplate reader (Varioskan Flash, Thermo Fisher Scientific, USA). For the in vitro aspirin release experiment, twenty milligrams of electrospinning membranes were placed in test tubes, immersed in 3 mL of PBS, and kept in a 37 °C-incubator shaker. At predetermined time intervals, all of the release medium was collected and replaced with an equal amount of fresh PBS. Because aspirin can be gradually hydrolyzed into salicylic acid in water, both unhydrolyzed aspirin and hydrolyzed aspirin (salicylic acid) in the release medium were measured to investigate the extent of aspirin release. Concentrations of unhydrolyzed aspirin were assayed by a multimode microplate reader (Varioskan Flash, Thermo Fisher Scientific, USA) at 278 nm, while salicylic acid concentration was measured at 298 nm. The amount of hydrolyzed aspirin was calculated by the following equation [39]:

$$\text{Hydrolyzed aspirin (mg)} = \frac{\text{salicylic acid (mg)}}{\text{molecular weight of salicylic acid (138.123 g/mol)}} \times \text{molecular weight of aspirin (180.160 g/mol).}$$

The total amount of released aspirin is equal to the sum of the unhydrolyzed aspirin and the hydrolyzed aspirin that we measured in the release medium.

Cell isolation and culture

DPSCs were used for the cell proliferation, cell-membrane attachment and cell differentiation assays. DPSCs were isolated from healthy third molars, which were removed from young donors (18–26 years old) at Hospital of Beihang University, with informed consent of each patient. Cell isolation procedures were conducted as previously

described [40]. All procedures conformed to the Declaration of Helsinki and were approved by the ethics committee of Beihang University. Isolated cells were cultured using α-minimum essential medium (α-MEM, Gibco, USA) supplemented with 10% fetal bovine serum (FBS, Gibco, USA), 100 U/mL penicillin, and 100 μg/mL streptomycin at 37 °C in a humidified atmosphere of 5% CO_2. The medium was changed every 2–3 days. When the cells reached 90% confluence, they were detached with a 0.25% trypsin-ethylenediaminetetraacetic acid solution (Solarbio, China), centrifuged, and resuspended in α-MEM for further experiments. DPSCs at passage 3 were used in this study. PAA and PLGA-PAA membranes were set as two experimental groups, while PLA membrane without aspirin and ACP served as the control group. Membranes were exposed under ultraviolet light for 6 h, immersed in 75% alcohol for 30 min, and washed with PBS 3 times before use.

Cell proliferation assays

A cell counting kit-8 (CCK-8, Dojindo Laboratory, Japan) was used to assess cell proliferation. DPSCs were seeded onto membranes (10 mg) in a 24-well plate at a density of 1×10^4 cells/well with 1 mL of culture medium. After 1, 3 and 5 days of culture, the culture medium was removed and 500 μL of fresh α-MEM containing 50 μL of CCK-8 solution was added to each well. After incubation at 37 °C in 5% CO_2 for 1 h, 100 μL of supernatant was collected and transferred to a 96-well plate. Absorbance was measured at 450 nm to assess cell proliferation using a multimode microplate reader (Varioskan Flash, Thermo Fisher Scientific, USA).

Acridine Orange/Ethidium Bromide (AO/EB) staining was used for assessment of cell morphology. Briefly, 500 μL of PBS containing 1 μg/mL AO (Solarbio, China) and 1 μg/mL EB (Solarbio, China) was added to each well. After 5 min incubation under room temperature, cells were washed with fresh PBS and examined under a fluorescence microscope (IX73, Olympus, Japan).

Cell-Electrospun membrane attachment assays

Cell-Electrospun membrane attachment was assessed according to previously described methods [41]. Briefly, DPSCs were seeded onto membranes in a 24-well plate at a density of 1×10^5 cells/well with 1 mL of culture medium. After co-culture for 5 h, membranes were washed with PBS three times. Next, cells still attached to the membranes were disassociated using 0.25% trypsin-ethylenediaminetetraacetic acid solution and counted using hemocytometer.

Cell differentiation ability assays

Alkaline phosphatase activity (ALP) assay and Alizarin red S (ARS) staining were employed for assays of cell differentiation ability. DPSCs were seeded onto membranes in a 24-well plate at a density of 1×10^4 cells/well. The culture medium was replaced by a differentiation medium consisting of α-MEM, 10% FBS, 100 U/mL penicillin, 100 μg/mL streptomycin, 50 μM L-ascorbic acid (Solarbio, China), 10 mM sodium β-glycerol phosphate (Solarbio, China) and 100 nM dexamethasone (Sigma-Aldrich, USA). The medium was changed every 2–3 days. At pre-determined times, the cellular sample in each well was washed three times in PBS.

ALP assays were conducted on day 7 and day 14. Briefly, cells were lysed with 70 μL of RIPA buffer containing 0.7 μL of protease inhibitor cocktail over an ice bath for 5 h. The cell lysate was then centrifuged and the supernatant was collected. ALP activity and total protein content in the supernatant was measured using an ALP assay kit (Nanjing Jiancheng, China) and a micro-BCA kit (Cwbiotech, China), respectively.

ARS staining was conducted on day 21. Briefly, cells were fixed in glutaraldehyde (2.5% in PBS) for 0.5 h and washed with distilled water. ARS staining solution (Solarbio, China) was added to each well and incubated with cells for 20 min under room temperature. Next, cells were washed five times with distilled water. The wells were photographed using a light microscope at 4 times magnification (Nikon Eclipse LV100ND, Japan).

In vitro anti-inflammation assay

Human monocytic THP-1 cells purchased from the American Type Culture Collection (ATCC, USA) were used for in vitro anti-inflammation assays. Cells were cultured using RPMI 1640 medium (Gibco, USA) supplemented with 10% FBS (Gibco, USA), 100 U/mL penicillin, and 100 μg/mL streptomycin at 37 °C in a humidified atmosphere of 5% CO_2. The medium was changed every 2–3 days.

For the anti-inflammation assay, THP-1 cells were first seeded onto a 24-well plate at a density of 1.5×10^5 cells/well. Next, cells were treated with phorbol 12-myristate 13-acetate (PMA, 50 ng/mL) (Sigma-Aldrich, USA) for 48 h to induce differentiation to macrophages. After washing with PBS three times to remove PMA, PLA, PAA, and PLGA-PAA membranes were added to each well along with fresh RPMI 1640 medium supplemented with lipopolysaccharide (LPS, 1 μg/mL) (Sigma-Aldrich, USA). Cells cultured only with LPS were set as positive controls. After 24 h of co-culture, the supernatants were collected from each well. The amounts of TNF-α and IL-1β in the supernatants were tested using enzyme-linked immunosorbent assay (ELISA)

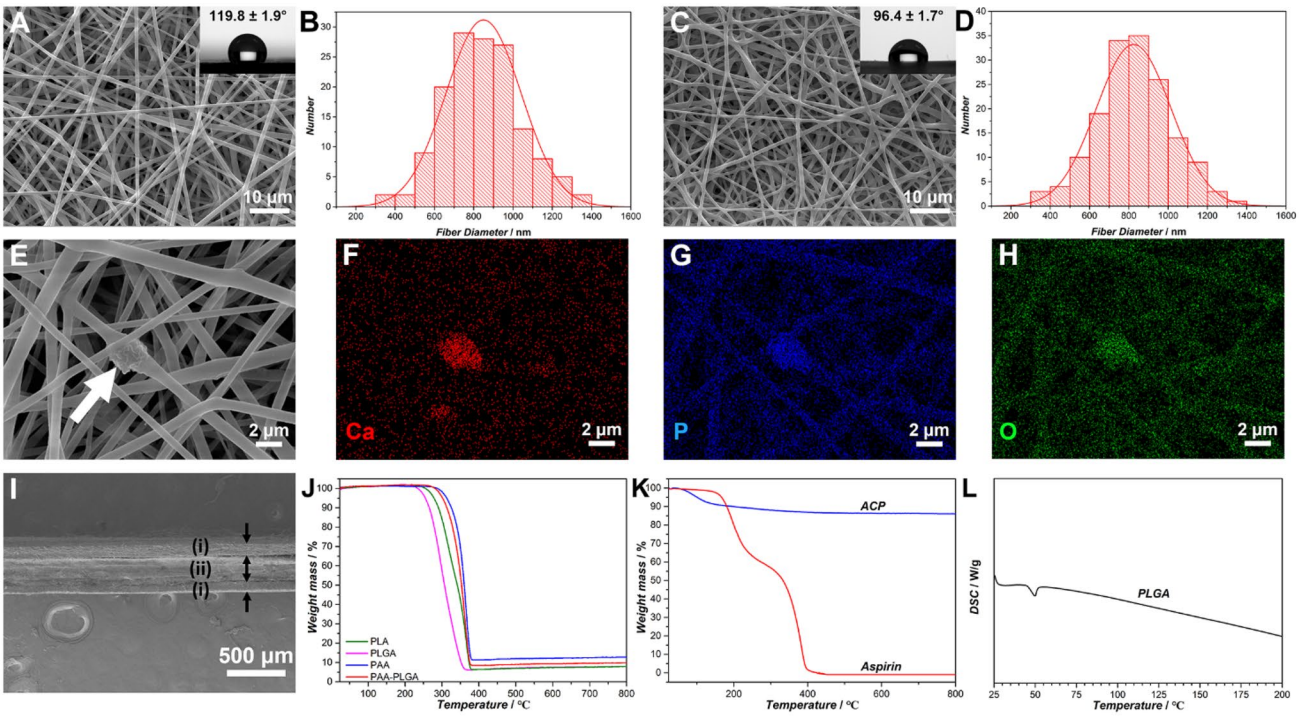

Fig. 1 SEM photographs, contact angle and diameter distribution histograms of PAA membrane (**a**, **b**) and PLGA-PAA membrane (**c**, **d**). **e**–**h** EDS mapping of specific PAA nanofibers with a rough surface. **i** Cross-section SEM image of a PLGA-PAA membrane. (i) PLGA membrane; (ii) PAA membrane. **j** TGA curves of PLA polymer, PLGA polymer, PAA membrane and PLGA-PAA membrane. **k** TGA curves of ACP and aspirin. **l** DSC curve of PLGA polymer

kits (Thermo Fisher Scientific, USA) to evaluate the anti-inflammatory ability of the membranes.

To evaluate long-term anti-inflammatory ability, another three groups of PLA, PAA and PLGA-PAA membranes were immersed in PBS for 18 days to simulate membranes that were implanted into the body for 18 days. These membranes were then co-cultured with LPS and differentiated THP-1 cells for the TNF-α and IL-1β expression assay.

Statistical analysis

All quantitative data are presented as mean ± standard deviation (SD). Statistical analysis was carried out using a one-way analysis of variance (ANOVA) and the statistical software package SPSS (IBM, USA). Statistical significance was defined as $p < 0.05$.

Results

Characterization of electrospinning membranes

Figures 1a–1d show the surface morphology and the corresponding fiber diameter distributions of PAA and PLGA-PAA membranes. Both membranes contained smooth and continuous nanofibers. The average diameter of PAA nanofibers was 849.8 ± 191.9 nm, while that of PLGA nanofibers was 824.3 ± 189.8 nm. The contact angle of both membranes was also tested (see insets in Figs. 1a and 1c). The PAA membrane had a contact angle of 119.8° ± 1.9°, indicating poor hydrophilicity. After coating with PLGA nanofibers, the contact angle of the PLGA-PAA membrane was measured as 96.4° ± 1.7°, which is significantly lower ($p < 0.001$) than that of the PAA membrane, demonstrating pronounced hydrophilicity. Figure 1i shows a cross-section image of a PLGA-PAA membrane. It can be seen that the PAA membrane is well sandwiched between the two PLGA membranes. The average thicknesses of the PAA membranes and PLGA membranes were 226.9 ± 9.8 μm and 89.3 ± 6.7 μm, respectively.

Although most PAA nanofibers were smooth, some nanofibers showed a rough surface with protuberances on the fiber (Fig. 1e, white arrow). EDS mapping of these protuberances showed strong Ca, P and O signals at the protuberance site (Figs. 1f–1h), indicating that the protuberances represented aggregated ACP. The amount of ACP loaded in the membranes was calculated by TGA. Figure 1j presents the TGA curves of PLA polymer, PLGA polymer, PAA membrane and PLGA-PAA membrane. After the addition of ACP, residue rates were increased in both PAA

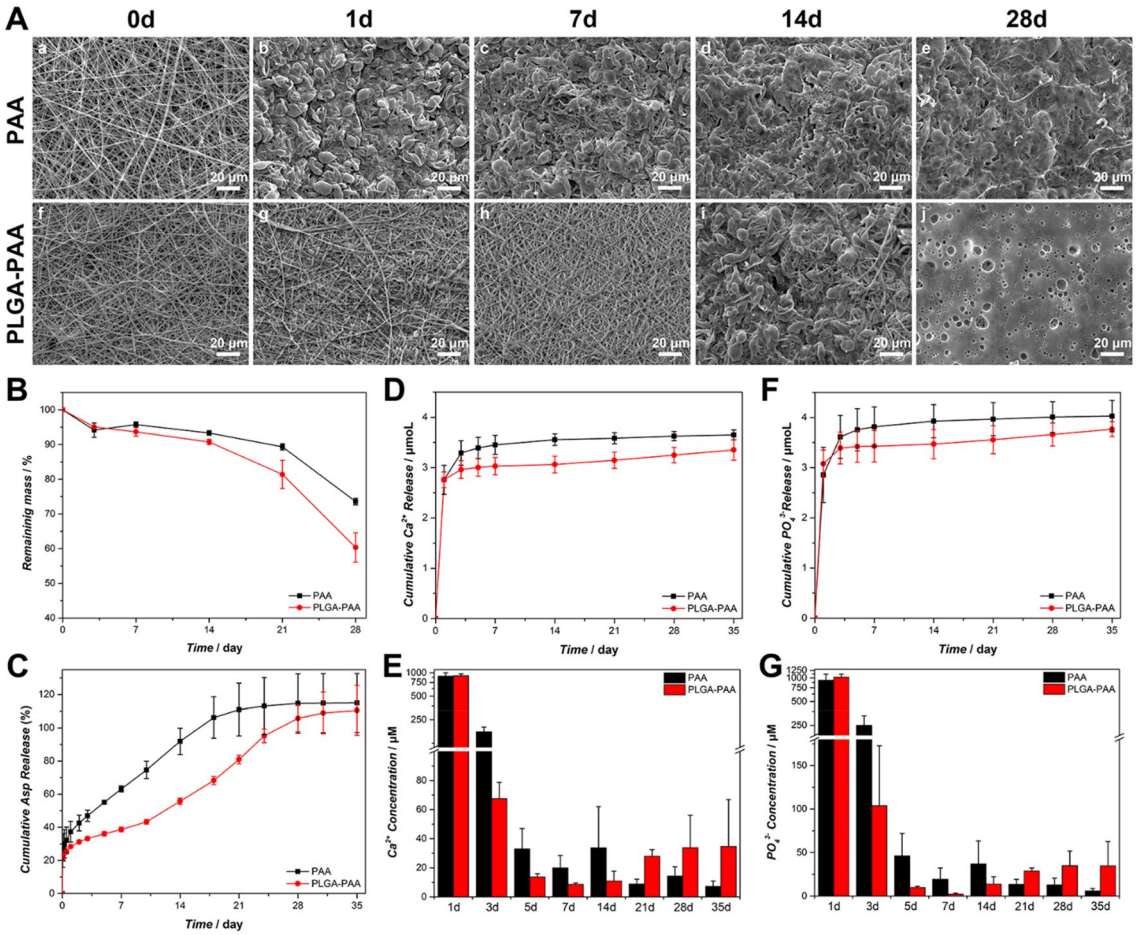

Fig. 2 SEM images (**A**) and mass loss (**B**) of PAA and PLGA-PAA membranes showing degradation over a period of 28 days. In vitro release profiles of aspirin (**C**), Ca^{2+} (**D**) and PO_4^{3-} (**F**) over a period of 35 days. **E** Ca^{2+} and **G** PO_4^{3-} concentrations in the release medium at various time points

membrane (12.84%) and PLGA-PAA membrane (9.85%), while the PLA polymer and PLGA polymer groups possessed similar lower residue rates of about 7.8%. To calculate the ACP loading amount more precisely, TGA curves of ACP and aspirin were also measured. Figure 1k shows that the residue rates of ACP and aspirin were 86.1% and 0%, respectively. Based on these data, we can calculate that the mass percentages of ACP in PAA and PLGA-PAA membranes were approximately 6.4% and 2.7%, respectively. Figure 1l further reveals that the PLGA we used here is an amorphous polymer with a glass transition temperature of about 45 °C.

In vitro degradation and release studies

In vitro release studies were carried out to investigate the effect of PLGA membranes on drug and ion release profiles of the electrospun membranes. Figure 2C shows the aspirin release profiles in vitro. It can be seen that approximately half of the aspirin was released from PAA membranes during the first 3 days, showing a strong initial burst of aspirin release. The SEM images indicate that the nanofiber structure of PAA membranes collapsed immediately on day 1 (Fig. 2A-b), which may account for the strong initial burst release. After 3 days, the aspirin release continued at a fast rate along with increasing destruction of nanofiber structure; all of the aspirin was released by day 18. In contrast, only 30% of the aspirin was released from the PLGA-PAA membrane initially, and aspirin release continued at a slow rate for the first 7 days. SEM observation revealed that the nanofiber network of the outer PLGA membrane layer gradually became denser during the first week. Before immersion in water, spaces can be easily found in the PLGA nanofiber network (Fig. 2A-f). After 1 day of immersion, however, most of the spaces had disappeared (Fig. 2A-g). After 7 days of immersion, almost no spaces could be seen inside the PLGA membrane (Fig. 2A-h), demonstrating good sealing properties.

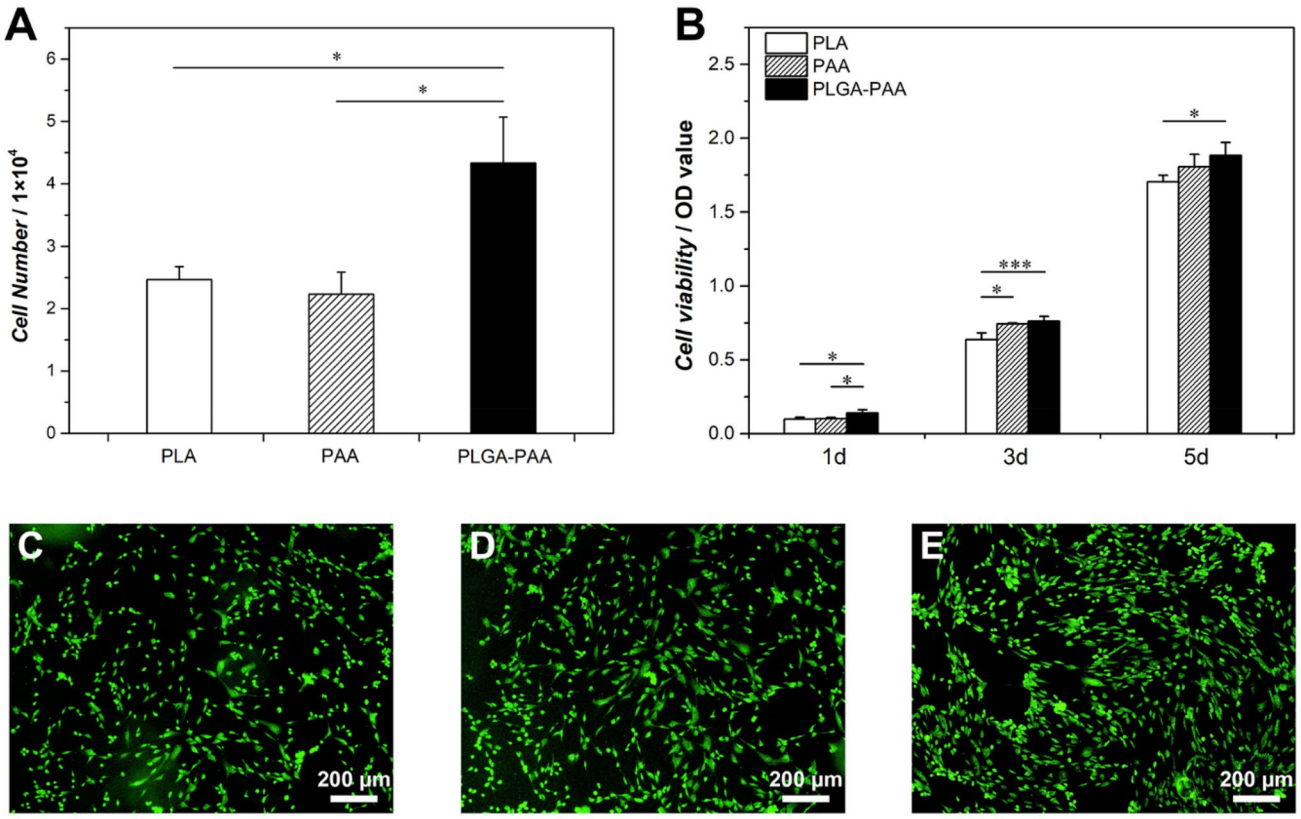

Fig. 3 DPSC attachment and proliferation assays. **a** DPSC attachment assays on different membranes. **b** CCK-8 assays of DPSC proliferation on different membranes. **c–e** AO/EB staining after 5 days of proliferation. **c** PLA membrane; **d** PAA membrane; **e** PLGA-PAA membrane. (* and *** denote the significant difference, $*p<0.05$; $***p<0.005$)

The PLGA membrane began to degrade on day 14, as seen by structural destruction of the PLGA nanofiber network (Fig. 2A-i) and accelerated mass loss from the PLGA-PAA membrane (Fig. 2B). Acceleration in aspirin release occurred along with the destruction of the PLGA layer. The aspirin release from the PLGA-PAA membrane lasted for 35 days, a period almost twice as long as that from the PAA membrane.

The PLGA-PAA membrane also inhibited an initial ion release, while prolonging the total ion release time when compared to that of the PAA membrane (Figs. 2D and 2F). However, compared with aspirin release, the initial burst release of ion was more obvious in both of the membranes. To characterize the pattern of ion release more precisely, the ion concentration was assayed at each time point (Figs. 2E and 2G). The ion release rate of the PAA membrane decreased over time, with little or no ion release after day 14. The ion release rate for the PLGA-PAA membrane also gradually decreased over the first 14 days. However, after day 14, the ion concentration increased in the PLGA-PAA group more steeply than that in the PAA group, showing a similar accelerated release pattern compared with that of aspirin release. Ca^{2+} and PO_4^{3-} ions can still be detected in the PLGA-PAA membrane group at relatively high concentrations on day 35.

In vitro cell attachment and viability assays

Cell attachment and viability assays were conducted to evaluate the biocompatibility of different membranes in vitro. Figure 3a shows that after 5 h of co-culture, a similar and relatively low cell attachment numbers (approximately 2.5×10^4 per membrane) were observed on both the PLA and PAA membranes. In comparison, PLGA-PAA membranes showed a significantly higher cell attachment number (approximately 4.3×10^4 per membrane), which is almost twice that of the other two membranes, demonstrating the superior cell adhesion properties of the PLGA-PAA membranes in early stages. CCK-8 assays (Fig. 3b) also show that cell proliferation viability in the PLGA-PAA group was significantly higher than that in the PLA ($p=0.014315$) and PAA ($p=0.019067$) group at the early stage (day 1), which is consistent with the cell attachment results. It can be seen from Fig. 3b that the PLGA-PAA membrane significantly facilitated cell proliferation at all time points when compared to the PLA membrane, while the cell proliferation

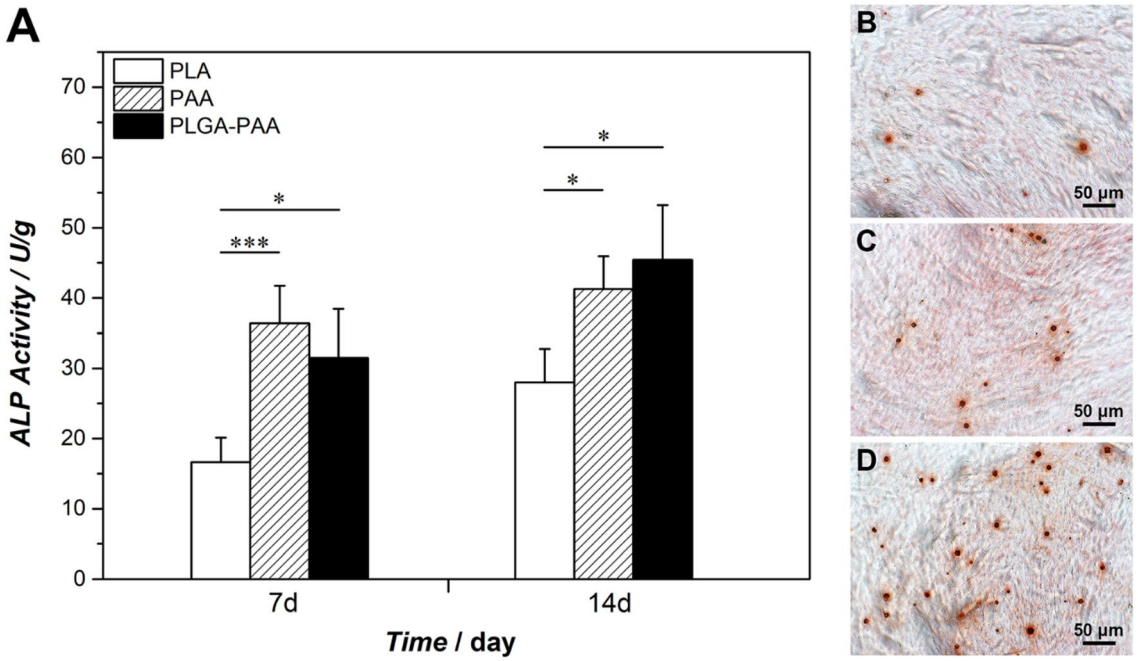

Fig. 4 In vitro DPSC differentiation assays. **a** ALP activity assays of DPSCs cultured on different membranes. **b–d** ARS staining of DPSCs after 21 days co-culture with different membranes. **b** PLA membrane; **c** PAA membrane; **d** PLGA-PAA membrane. (* and *** denote the significant difference, $*p < 0.05$; $***p < 0.005$)

viability in the PAA group was only significantly higher than that in the PLA group on day 3; for the rest of the experimental period, the PAA and PLA groups exhibited comparable effects on cell proliferation. AO/EB staining (Figs. 3c–3e) further revealed that after 5 days of proliferation, cells in all groups exhibited good morphology regardless of proliferation rate.

In vitro cell differentiation assays

ACP has been shown to effectively promote cell osteogenic differentiation, as it can be converted in aqueous solution to HA with sustained release of Ca^{2+} and PO_4^{3-} ions. For this reason, we carried out additional analysis of the osteogenic differentiation performance of DPSCs on different membranes. Figure 4a shows ALP activity in DPSCs after 7 and 14 days of co-culture with different membranes. It can be seen that ALP activity significantly increased in the PAA and PLGA-PAA membranes compared to that in the PLA membrane, indicating the effectiveness of ACP on osteogenic differentiation. In order to confirm this finding, ARS staining was conducted to identify the formation of mineralized matrix, i.e., calcium deposition, in different groups. After 21 days of co-culture, the highest amount of calcium deposition was found in the PLGA-PAA group (Fig. 4d), while the lowest amount of calcium deposition was observed in the PLA group (Fig. 4b). The PAA group showed an intermediate level of calcium deposition, lower than that of the PLGA-PAA group and higher than in the PLA group.

In vitro anti-inflammation studies

As a classic nonsteroidal anti-inflammatory drug, aspirin is well known for its anti-inflammatory properties. Here, we investigated the expression of TNF-α and IL-1β, two typical pro-inflammatory cytokines, in LPS-stimulated macrophages to evaluate the anti-inflammatory effects of different membranes. When cells were co-cultured on membranes without pre-immersion (Fig. 5a), the expression of TNF-α and IL-1β was significantly down-regulated in the PAA and PLGA-PAA groups, while the expression level of these cytokines in the PLA group was similar to that of the control group (cells cultured with LPS only).

As shown in Fig. 2C, the outer layer of the PLGA membrane can potentially prolong aspirin release of the PLGA-PAA membrane. Thus, membranes pre-immersed in PBS for 18 days were also co-cultured with cells to assess their long-term anti-inflammatory effects. For cells co-cultured with membranes after 18 days of pre-immersion, only the PLGA-PAA group showed significantly decreased secretion of TNF-α and IL-1β compared with that of the other three groups (Fig. 5b), indicating the long-term inhibitory effect of the PLGA membrane on the expression of these two pro-inflammatory cytokines.

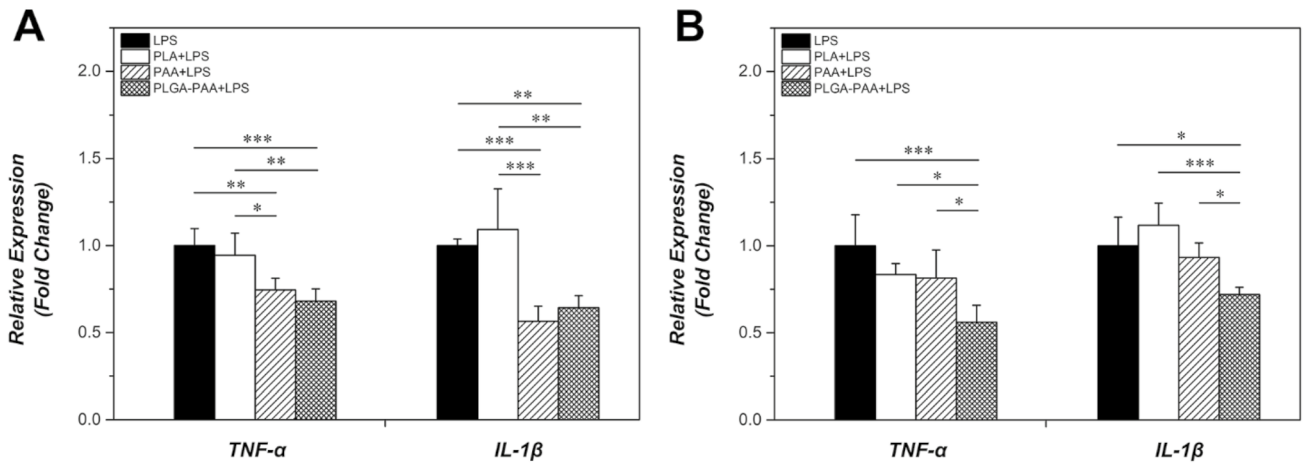

Fig. 5 In vitro anti-inflammation assays of different membranes tested by ELISA. Membranes without pre-immersion were used to evaluate the early anti-inflammatory effects, while membranes pre-immersed in PBS for 18 days were used to evaluate the long-term anti-inflammatory effects. **a** TNF-α and IL-1β expression at 24 h after treatment with membranes without pre-immersion. **b** TNF-α and IL-1β expression at 24 h after treatment with membranes pre-immersed in PBS for 18 days. THP-1 derived macrophages treated with LPS were set as the control group. (*, ** and *** denote the significant difference, $*p<0.05$; $**p<0.01$; $***p<0.005$)

Discussion

Recently, many kinds of electrospun membranes have been fabricated and used as pulp-capping materials. In these studies, drugs and mineral components have been loaded onto the membranes, and these membranes have achieved some success in dental pulp regeneration. However, owing to the single-layered structure of these membranes, the period of drug release in these membranes is always limited to a few hours or a few days [1], which is too short a time period for dental pulp regeneration. Some studies only add mineral components to the electrospun membranes [2], while ignoring the addition of anti-inflammatory drugs. The absence of anti-inflammatory agents may cause persistent local inflammation inside the tooth, with negative effects on dentin formation. In this study, we have developed a novel PLGA-PAA membrane using a multilayering electrospinning technique to create a new type of pulp-capping material. Different from the traditional single-layer electrospun membrane, our design contains three electrospun layers in the PLGA-PAA membrane, with the PAA layer sandwiched between two PLGA layers, forming a sandwich-like structure. We hypothesized that aspirin and ion release from PAA membrane are inhibited not only by the PLA nanofibers, but also by the PLGA electrospun membranes, enabling this PLGA-PAA membrane could achieve a capability for sustained aspirin and ion release and long-term anti-inflammatory effects that are favorable for dental pulp regeneration.

To better validate release-inhibition effect of PLGA membrane, low molecular weight PLA was chosen to fabricate a PAA membrane with fast release rate. During the entire membrane-degradation and release period in vitro, PAA membrane and PLGA-PAA membrane exhibit different surface-morphologies and release patterns. In the PAA membrane, the PLA nanofiber structure collapses immediately after being immersed in water, resulting in fast release of aspirin and ions within the first few days, while the two PLGA membrane layers in the sandwich-like structure of the PLGA-PAA membrane provide an inhibitory effect on aspirin and ion release. Unlike the PAA membrane, the outer PLGA membrane layers in the PLGA-PAA membrane maintain their nanofiber structure after immersion, and the PLGA nanofiber network becomes gradually denser over time. By day 7, no spaces can be found in the nanofiber network, indicating that the PLGA membrane has reached its maximum release-inhibition effect. Thus, a gradually decreased aspirin release rate is observed in the first week.

A possible mechanism explaining the release-inhibition effect of the PLGA membrane is illustrated in Fig. 6. Before being immersed in water, PLGA fibers are straight and exhibit a nano-dimensional structure with many internal spaces. This is caused by the electric field during the electrospinning process, which regulates the orientation and alignment of molecular chains within the electrospun fibers [42]. At this time, the existence of spaces limits the release-inhibition effect of the PLGA membrane. After immersion in water at 37 °C (an environment with high temperature and humidity), the molecular chains within the PLGA fibers rapidly relax to a random coil state because of the inherently amorphous property of PLGA (Fig. 1l) [43]. As a result, the dimensional shrinkage of the PLGA membrane occurs, and its nanofiber network becomes dense, with only a few

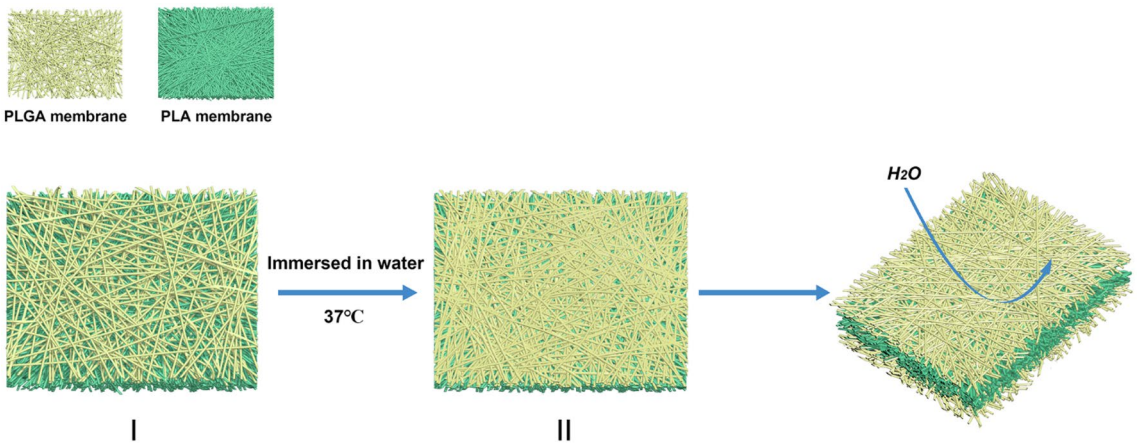

Fig. 6 Schematic illustration of the proposed mechanism for the release-inhibition effect of PLGA membranes. Stage I: PLGA-PAA membrane before immersion in water. Spaces can be found inside the nanofiber network of PLGA membrane. Stage II: After immersion in water, PLGA chains relax rapidly to a random-coil state, causing dimensional shrinkage of the PLGA membrane, which results in formation of a dense nanofiber network. Owing to this, spaces are rarely observed on the surface of the PLGA membrane and water cannot easily penetrate into the innermost region, i.e., the PAA membrane, which is sandwiched between two PLGA membranes

remaining spaces. Thus, water cannot easily penetrate into the inner part of the PLGA-PAA membrane and elute the drug in the innermost layer.

It should be noted that after the slow release of aspirin in the first few days, an acceleration of aspirin release is observed in the PLGA-PAA group on day 14. We believe that this acceleration is caused by degradation of the polymers, which destroys the structural integrity of the PLGA membrane. As both a sharp drop in mass (Fig. 2B) and destruction of fiber structure (Fig. 2A-i) are observed in the PLGA-PAA group in this time period. Compared with the PAA membrane, the PLGA-PAA membrane finally doubles the aspirin release time in vitro.

Ion release has a similar release pattern to that of aspirin release except for the obvious initial burst release. From our previous study we know that the Ca^{2+} and PO_4^{3-} ions in the release medium originate from the conversion of ACP to hydroxyapatite (HA) in aqueous solution, and the conversion process occurs mainly in the first 9 h [32]. In this study, the PLGA membrane, which plays a major role in inhibiting release, was not able to achieve its maximum inhibition effect until day 7. On day 1, spaces can still be found in the nanofiber network. However, at this time, most of the conversion from ACP to HA has been already completed. Thus, the inhibitory effect of PLGA membranes on ion release is weaker than that on aspirin release, resulting in the notably initial burst release of Ca^{2+} and PO_4^{3-} ions.

Regeneration of the dentin-pulp complex is known to be a long-term process, and dentin formation and pulp regeneration are the most important components of that process. Thus, electrospun membranes used for dentin-pulp complex regeneration should have the ability to promote osteogenesis as well as provide long-term anti-inflammatory effects. The in vitro cell proliferation and differentiation assays conducted here demonstrate that DPSCs attach to PLGA-PAA membranes more quickly than to the other two membrane types, as the PLGA membrane improves the superficial hydrophilicity of the membrane. This hydrophilic property also improves the biocompatibility of PLGA-PAA membrane, increasing also its favorability for cell proliferation. During the 5 days of proliferation, the PLGA-PAA group showed the highest cell viability at all time points. Subsequent cell osteogenic differentiation assays showed that the PAA and PLGA-PAA groups possess comparable ALP activity on both day 7 and day 14. This apparent lack of advantage for the PLGA-PAA membrane could be explained by the weak inhibitory effect of the PLGA membrane on ion release, which creates a similar ion release pattern in these two groups in the first 14 days, finally resulting in a similar ALP activity. ARS staining was also conducted to validate the effects of different membranes on cell osteogenic differentiation. After 21 days of co-cultivation, both the PLGA-PAA membrane and PAA membrane showed significantly higher rates of calcium deposition compared to that of PLA membrane. It should also be noted that the amount of calcium deposition in PLGA-PAA membrane is higher than that of PAA membrane at day 21. We suspect that this difference is caused by a second wave of ion release that we observed in the PLGA-PAA group around day 14, which would increase Ca^{2+}/PO_4^{3-} concentrations in the culture medium and promote cell differentiation.

After injury, there will always be a chronic inflammatory reaction in the exposed pulp site. It is well known that long-term inflammatory reactions are not only harmful to restoring the viability of pulp tissue; they also have adverse effects on dentin formation. For this reason, we compared the anti-inflammatory abilities of different electrospun membranes in this study. We first co-cultured THP-1 cells on membranes without pre-immersion to simulate the immediate anti-inflammatory effect of membranes after implantation. These results showed that both PAA and PLGA-PAA membranes can suppress the expression of pro-inflammatory cytokines. Subsequently, THP-1 cells were co-cultured on membranes pre-immersed in PBS for 18 days to simulate the long-term anti-inflammatory effects of membranes after implantation. Of the membrane types test, only the PLGA-PAA membrane showed significantly lower expression of pro-inflammatory cytokines compared to the other three groups. Our in vitro aspirin release studies suggest that these differences in cytokine expression are caused by the different aspirin release patterns observed in these groups. For PAA membrane, almost all the aspirin was released from the PAA membrane in the first 18 days. While at this time point, more than 30% of the aspirin was still retained in the PLGA-PAA membrane. As shown in Fig. 2C, residual aspirin in PLGA-PAA membrane can be gradually released until day 35, indicating that the outer layer of the PLGA membrane might be able to double the period of anti-inflammatory effects generated by the inner PAA layer of the PLGA-PAA membrane.

Conclusions

A PLGA-PAA sandwich-structured membrane has been fabricated using a multilayering electrospinning technique and tested as a novel pulp capping material. The PLGA electrospun membranes coating both sides of a PAA membrane slightly slow down ion release, and significantly prolong aspirin release. The outer PLGA membrane layers also elevate the hydrophilicity of the PAA membrane, thus promoting cell adhesion, and cell proliferation in the early stage. Finally, co-culture experiments with electrospun membranes and cells indicate that the PLGA-PAA membrane promotes osteogenic differentiation, with long-term anti-inflammatory effects lasting at least 18 days. The present PLGA-PAA electrospun membrane has the ability to promote dentin formation while suppress inflammation over a long period of time, suggesting its potential applications in dental pulp regeneration and repair of other bone defects.

Acknowledgements The authors gratefully acknowledge the financial support from the National Natural Science Foundation of China (Nos. 11872097, 82074463, 11827803, and U20A20390), the National Key R&D Program of China (No. 2020YFC0122204), the 111 Project (No. B13003), and the International Joint Research Center of Aerospace Biotechnology and Medical Engineering, Ministry of Science and Technology of China.

Author contributions FHY and XFN contributed to conceptualization; FHY, JXW, XYL, and ZZJ contributed to methodology; FHY contributed to investigation; FHY contributed to writing—original draft; QW, DZY, JYL, and XFN contributed to writing—review & editing; XFN contributed to funding acquisition; XFN provided the resources; JYL and XFN contributed to supervision.

Declarations

Conflict of interest The authors declare that there is no conflict of interest.

Ethical approval This study does not contain any studies with human or animal subjects performed by any of the authors.

References

1. Tort H, Oktay EA, Tort S et al (2017) Evaluation of ornidazole-loaded nanofibers as an alternative material for direct pulp capping. J Drug Deliv Sci Technol 41:317–324. https://doi.org/10.1016/j.jddst.2017.07.010
2. Lee W, Oh JH, Park JC et al (2012) Performance of electrospun poly(epsilon-caprolactone) fiber meshes used with mineral trioxide aggregates in a pulp capping procedure. Acta Biomater 8(8):2986–2995. https://doi.org/10.1016/j.actbio.2012.04.032
3. Wang J, Liu X, Jin X et al (2010) The odontogenic differentiation of human dental pulp stem cells on nanofibrous poly(L-lactic acid) scaffolds in vitro and in vivo. Acta Biomater 6(10):3856–3863. https://doi.org/10.1016/j.actbio.2010.04.009
4. Lee LW, Hsiao SH, Hung WC et al (2015) Clinical outcomes for teeth treated with electrospun poly(epsilon-caprolactone) fiber meshes/mineral trioxide aggregate direct pulp capping. J Endod 41(5):628–636. https://doi.org/10.1016/j.joen.2015.01.007
5. Choung HW, Lee DS, Lee JH et al (2016) Tertiary dentin formation after indirect pulp capping using protein CPNE7. J Dent Res 95(8):906–912. https://doi.org/10.1177/0022034516639919
6. Peycheva K (2015) Pulp-capping with mineral trioxide aggregate. Acta Med Bulgarica 42(2):23–29. https://doi.org/10.1515/amb-2015-0014
7. Furey A, Hjelmhaug J, Lobner D (2010) Toxicity of flow line, durafill vs, and dycal to dental pulp cells: effects of growth factors. J Endod 36(7):1149–1153. https://doi.org/10.1016/j.joen.2010.03.013
8. Parirokh M, Torabinejad M, Dummer PMH (2018) Mineral trioxide aggregate and other bioactive endodontic cements: an updated overview—part I: vital pulp therapy. Int Endod J 51(2):177–205. https://doi.org/10.1111/iej.12841
9. da Rosa WLO, Cocco AR, da Silva TM et al (2018) Current trends and future perspectives of dental pulp capping materials: a systematic review. J Biomed Mater Res B 106(3):1358–1368. https://doi.org/10.1002/jbm.b.33934
10. Brizuela C, Ormeno A, Cabrera C et al (2017) Direct pulp capping with calcium hydroxide, mineral trioxide aggregate, and biodentine in permanent young teeth with caries: a randomized clinical trial. J Endod 43(11):1776–1780. https://doi.org/10.1016/j.joen.2017.06.031

11. Torabinejad M, Parirokh M (2010) Mineral trioxide aggregate: a comprehensive literature review-part II: leakage and biocompatibility investigations. J Endod 36(2):190–202. https://doi.org/10.1016/j.joen.2009.09.010
12. Palma PJ, Marques JA, Falacho RI et al (2019) Six-month color stability assessment of two calcium silicate-based cements used in regenerative endodontic procedures. J Funct Biomater 10(1):14. https://doi.org/10.3390/jfb10010014
13. Hilton TJ (2009) Keys to clinical success with pulp capping: a review of the literature. Oper Dent 34(5):615–625. https://doi.org/10.2341/09-132-0
14. Sanaei-rad P, Jamshidi D, Adel M et al (2021) Electrospun poly(L-lactide) nanofibers coated with mineral trioxide aggregate enhance odontogenic differentiation of dental pulp stem cells. Polym Adv Technol 32(1):402–410. https://doi.org/10.1002/pat.5095
15. Daghrery A, Aytac Z, Dubey N et al (2020) Electrospinning of dexamethasone/cyclodextrin inclusion complex polymer fibers for dental pulp therapy. Colloids Surf B Biointerface 191:111011. https://doi.org/10.1016/j.colsurfb.2020.111011
16. Thakor J, Ahadian S, Niakan A et al (2020) Engineered hydrogels for brain tumor culture and therapy. Bio-Des Manuf 3(3):203–226. https://doi.org/10.1007/s42242-020-00084-6
17. Ma PX (2004) Scaffolds for tissue fabrication. Mater Today 7(5):30–40. https://doi.org/10.1016/S1369-7021(04)00233-0
18. Song JQ, Zhu GL, Gao HC et al (2018) Origami meets electrospinning: a new strategy for 3D nanofiber scaffolds. Bio-Des Manuf 1(4):254–264. https://doi.org/10.1007/s42242-018-0027-9
19. Gao Q, Zhao P, Zhou RJ et al (2019) Rapid assembling organ prototypes with controllable cell-laden multi-scale sheets. Bio-Des Manuf 2(1):1–9. https://doi.org/10.1007/s42242-019-00032-z
20. Li Z, Du T, Ruan C et al (2021) Bioinspired mineralized collagen scaffolds for bone tissue engineering. Bioact Mater 6(5):1491–1511. https://doi.org/10.1016/j.bioactmat.2020.11.004
21. Song W, Chen L, Seta J et al (2017) Corona discharge: a novel approach to fabricate three-dimensional electrospun nanofibers for bone tissue engineering. ACS Biomater Sci Eng 3(6):1146–1153. https://doi.org/10.1021/acsbiomaterials.7b00061
22. Kost B, Svyntkivska M, Brzezinski M et al (2020) PLA/beta-CD-based fibres loaded with quercetin as potential antibacterial dressing materials. Colloids Surf B Biointerface. https://doi.org/10.1016/j.colsurfb.2020.110949
23. Konwarh R (2019) Can the venerated silk be the next-generation nanobiomaterial for biomedical-device designing, regenerative medicine and drug delivery? Prospects and hitches. Bio-Des Manuf 2(4):278–286. https://doi.org/10.1007/s42242-019-00052-9
24. Niu X, Liu Z, Hu J et al (2016) Microspheres assembled from chitosan-graft-poly(lactic acid) micelle-like core-shell nanospheres for distinctly controlled release of hydrophobic and hydrophilic biomolecules. Macromol Biosci 16(7):1039–1047. https://doi.org/10.1002/mabi.201600020
25. Loi F, Cordova LA, Pajarinen J et al (2016) Inflammation, fracture and bone repair. Bone 86:119–130. https://doi.org/10.1016/j.bone.2016.02.020
26. Claes L, Recknagel S, Ignatius A (2012) Fracture healing under healthy and inflammatory conditions. Nat Rev Rheumatol 8(3):133–143. https://doi.org/10.1038/nrrheum.2012.1
27. Sun L, Li X, Xu M et al (2020) In vitro immunomodulation of magnesium on monocytic cell toward anti-inflammatory macrophages. Regen Biomater 7(4):391–401. https://doi.org/10.1093/rb/rbaa010
28. Mahon OR, Browe DC, Gonzalez-Fernandez T et al (2020) Nanoparticle mediated M2 macrophage polarization enhances bone formation and MSC osteogenesis in an IL-10 dependent manner. Biomaterials 239:119833. https://doi.org/10.1016/j.biomaterials.2020.119833
29. Yang F, Niu X, Gu X et al (2019) Biodegradable magnesium-incorporated poly(L-lactic acid) microspheres for manipulation of drug release and alleviation of inflammatory response. ACS Appl Mater Interface 11(26):23546–23557. https://doi.org/10.1021/acsami.9b03766
30. Tamaddon M, Wang L, Liu Z et al (2018) Osteochondral tissue repair in osteoarthritic joints: clinical challenges and opportunities in tissue engineering. Bio-Des Manuf 1(2):101–114. https://doi.org/10.1007/s42242-018-0015-0
31. Niu X, Liu Z, Tian F et al (2017) Sustained delivery of calcium and orthophosphate ions from amorphous calcium phosphate and poly(L-lactic acid)-based electrospinning nanofibrous scaffold. Sci Rep. https://doi.org/10.1038/srep45655
32. Niu X, Chen S, Tian F et al (2017) Hydrolytic conversion of amorphous calcium phosphate into apatite accompanied by sustained calcium and orthophosphate ions release. Mater Sci Eng C 70:1120–1124. https://doi.org/10.1016/j.msec.2016.04.095
33. Kotsakis GA, Thai A, Ioannou AL et al (2015) Association between low-dose aspirin and periodontal disease: results from the continuous national health and nutrition examination survey (NHANES) 2011–2012. J Clin Periodontol 42(4):333–341. https://doi.org/10.1111/jcpe.12380
34. Xu X, Zhang K, Zhao L et al (2016) Aspirin-based carbon dots, a good biocompatibility of material applied for bioimaging and anti-inflammation. ACS Appl Mater Interface 8(48):32706–32716. https://doi.org/10.1021/acsami.6b12252
35. Kidoaki S, Kwon IK, Matsuda T (2005) Mesoscopic spatial designs of nano- and microfiber meshes for tissue-engineering matrix and scaffold based on newly devised multilayering and mixing electrospinning techniques. Biomaterials 26(1):37–46. https://doi.org/10.1016/j.biomaterials.2004.01.063
36. Laha A, Sharma CS, Majumdar S (2017) Sustained drug release from multi-layered sequentially crosslinked electrospun gelatin nanofiber mesh. Mater Sci Eng C 76:782–786. https://doi.org/10.1016/j.msec.2017.03.110
37. Okuda T, Tominaga K, Kidoaki S (2010) Time-programmed dual release formulation by multilayered drug-loaded nanofiber meshes. J Contr Release 143(2):258–264. https://doi.org/10.1016/j.jconrel.2009.12.029
38. Kim K, Yu M, Zong XH et al (2003) Control of degradation rate and hydrophilicity in electrospun non-woven poly(D, L-lactide) nanofiber scaffolds for biomedical applications. Biomaterials 24(27):4977–4985. https://doi.org/10.1016/s0142-9612(03)00407-1
39. Tang Y, Singh J (2008) Controlled delivery of aspirin: effect of aspirin on polymer degradation and in vitro release from PLGA based phase sensitive systems. Int J Pharm 357(1–2):119–125. https://doi.org/10.1016/j.ijpharm.2008.01.053
40. Zheng L, Zhang L, Chen L et al (2018) Static magnetic field regulates proliferation, migration, differentiation, and YAP/TAZ activation of human dental pulp stem cells. Tissue Eng Regen Med 12(10):2029–2040. https://doi.org/10.1002/term.2737
41. Wei D, Qiao R, Dao J et al (2018) Soybean lecithin-mediated nanoporous PLGA microspheres with highly entrapped and controlled released BMP-2 as a stem cell platform. Small. https://doi.org/10.1002/smll.201800063
42. Cui W, Zhu X, Yang Y et al (2009) Evaluation of electrospun fibrous scaffolds of poly(DL-lactide) and poly(ethylene glycol) for skin tissue engineering. Mater Sci Eng C 29(6):1869–1876. https://doi.org/10.1016/j.msec.2009.02.013
43. Ru C, Wang F, Pang M et al (2015) Suspended, shrinkage-free, electrospun PLGA nanofibrous scaffold for skin tissue engineering. ACS Appl Mater Interface 7(20):10872–10877. https://doi.org/10.1021/acsami.5b01953